TJPS

TIKRIT JOURNAL OF PURE SCIENCE

Journal Homepage: http://main.tu-jo.com/ojs/index.php/TJPS/index

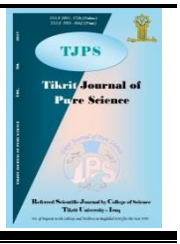

The effect of gold Nanoparticles on Structural and Electrical properties of WO_3 thin films

Niran F. Abdul-Jabbar[1], Issam M.Ibrahim[2], Abeer H. Fezaa[1]

[1]*Department of Physics, College of Education, University of Tikrit , Tikrit , Iraq*
[2]*Department of Physics, College of Science, University of Baghdad , Baghdad , Iraq*

ARTICLE INFO.

Article history:
-Received: 14 / 9 / 2017
-Accepted: 21 / 11 / 2017
-Available online: / / 2018

Keywords: Tungsten oxide, Au, structural properties, electrical properties, Chemical spray pyrolysis method.

Corresponding Author:

Name: Niran F. Abdul-Jabbar

E-mail:
Niranfadhil64@gmail.com

Tel:

Affiliation:

Abstract

Chemical spray pyrolysis technique was used at temperature 250˚C with annealing temperature at 400C˚(for 1hour) to deposition tungsten oxide thin film with different doping concentration of Au nanoparticle (0, 10, 20, 30 and 40) wt.% on glass substrate with thickness about 100 nm. The structural and electrical properties were investigated. The structure properties shows that the films at substrate by x-ray diffraction (XRD) temperature (250˚C) was amorphous structure while at annealing temperature have a polycrystalline structure with the preferred orientation of (200) , all the samples have a hexagonal structure for WO_3 and Au gold nanoparticles have a cubic structure .The mechanisms of dc-conductivity of un-doped WO_3 and doped with Au (10,20,30 and 40) wt.% thin films at the range (303 to 473) K have been discussed , there is decrease in conductivity with the increase in the doping concentration and hall measurements show that all films have a negative hall coefficient and n_H increases with the increase of Au dopant ratio and decreasing in carrier mobility (μ_H) with increasing of Au .

1- Introduction

Metal nanoparticles have been studied for decades as they have properties not found in the same material in bulk form. The nanosize effects greatly the ratio of surface atoms to atoms deep in the crystal matrix. Therefore, surface effects are observed to a much greater extent. A notable example is catalysis, where a large surface area to volume ratio is a key parameter [1] .The smooth surface of metals in bulk state presents a shiny appearance, and this behavior is attributed to the total reflection of light due to the high density of electrons in the material. Contrariwise, finely divided metals look dark, because the large surface absorbs light through repeated reflection phenomena [2].When metals reach nanometer size, strong absorption of light can happen when the frequency of the electromagnetic field becomes resonant with the coherent electron movement [3]. In the case of Au, Ag and Cu, which present free conduction electrons with plasma frequency in the visible region, nanoparticles appear colored [4]. Other transition metals, instead, show only broad and poorly resolved absorption bands in the ultraviolet region [3]. The color and optical properties of metal nanoparticles are due to the presence of a collective longitudinal excitation of conduction electrons on the surface of the nanoparticles, known as Surface Plasmon Resonance (SPR) [5].In this research the essential aim of work to prepare a pure WO_3 thin films and doped with Au by using chemical spray pyrolysis method at different concentration (0, 10, 20, 30 and 40) wt. % and study the structural and electrical properties of these prepared samples.

2- Experimental details

2-1 Sample preparation:

The solution was prepared by mixed HCl and H_2O_2 to get WCl_6 according to equation (1).The molar concentration of the solution must be equal to 0.05 mol / litter. To prepare the solution of 0.05 molar concentrations from these two materials, few grams weight are needed from each of them, heated 90 ml of distilled water, according to the following equation (2).

$$6\,HCL + H_2O_2 + H_2WO_4 \xrightarrow{\Delta} WCL_6 + 5H_2 + 3O_2 \ldots. \quad (1)$$

W (gm) =V (ml) × M (mol/l) ×M.W (gm/mol) … (2)

According to equation (2), the weight which is required from tungsten material can be calculated as following**:**

M .wt of WO_3= (231.84×0.05 ×100)/1000= 1.1592gm.

Where the molecular weight of the WO_3= 231.84 gm / mol

A digital balance type "Mettler AE- 160" with accuracy of 10^{-4} g is used for weighting the needed material.

Finally, the weight material heated in (100 ml) of distilled water to get the wanted solution. Then, it was putting on the magnetic stirrer for 15 minutes to be sure that the mixture solutions are well mixed. After then the solution was ready for using.

2-2 Thin Film Preparation of WO_3:

Chemical spray pyrolysis method , thin films were prepared by spraying the solution on a hot glass substrate at a temperature about (250˚C), and the film will be formed by the chemical reaction of the prepared solution on the hot substrate .To get the finally WO_3 thin film according to the following chemical equation [3].

$$2WCl_6 + 3O_2 \xrightarrow{\Delta} 2WO_3 + 6\,Cl_2 \text{ …. (3)}$$

It is necessary to leave the glass substrate on the electrical heater for one hour at least after finishing the operation of spraying to complete its oxidation and crystalline growth process. In the spray system, compressed and purified air was used as the carrier gas with a 3 kg / cm^2 pressure and the spraying solution 0.05 M concentration, the distance between the spray nozzle and the substrate was fixed at 22 cm the deposition rate is ~5 min, then the substrates can be raised.

2-3 Preparation of Au Nano Solution

Nanoparticles gold solution was prepared by (Nd-YAG Laser) type (HUAFEI) at a wavelength (1064 nm) and frequency of pulses (6 HZ), using removal by leaser inside solution . putting small pieces of high gold purity (99.99%) in glass container contains (2 ml) of distilled water. The distance between the target and laser beam was (12 cm) , the energy required for preparation was (500mJ) and the number of pulses (200 pulse) the time for preparation was (6 min). Many tests were used to examine the produced thin film such as XRD, D.C conductivity and Hall Effect.

3- Results and discussion

3-1 Structural analysis

Fig.(1) shows XRD patterns of WO_3 thin films with doping by gold nanoparticles as prepared at 250 ˚C were amorphous structure this results agree with Myong and et al [7] and with Ayat and et al [8] ,the addition of Au gold nanoparticles into WO_3 did not improve the structure of WO_3 up to Au concentration of 40% , as evidenced from the absence of XRD peaks, however ,at higher Au concentration (40%) there was still no improvement in the structure of WO_3, fig.(2)shows annealed films at 400˚C, many small and high peaks was showed in pure film are belongs to WO_3 this obtain that the film is a polycrystalline and the preferential orientation of the film was a long the plan (200) at diffraction angle of 2θ = 28.19˚ which in agreement with [7-9]. When the Au was added at ratio 10%, new one peak (200) was appeared belongs to Au at 2θ =44.41˚. An additional peak was appear (111) at 2θ =37.82˚ is also belongs to Au was showed in the ratio 20%. In the ratios 30% and 40% the intensity of peaks of Au becomes to increases and the peak's intensity of WO_3 gradually began to decrease ,all the samples have a hexagonal structure for WO_3 according to International Centre for Diffraction (card No.96-100-4058) ,and which is doped gold nanoparticles have a cubic structure according to the International Centre for Diffraction (96-901-2431) (see Table 1), in the randomly there are defects and levels of the tail and at annealing are improving the composition of the material and rearrangement, which led to conversion to multible crystallization its' mean removing some defects and gaps remained local levels and therefore the gap is less more than before. The crystallite size decreases by increasing the deflection, this is explained by the large diameter of the ion of the defect will be interface, which leads to the decrease in crystallite size and thus an increase of (2θ), the crystallite size is inversely propotional to the (FWHM) this is agree with[10-13], the average crystallite size was equal to (9.24)nm it was estimated with Debye – scherrer formula for the (200) reflection follow[14]:

$$D = \frac{0.94\,\lambda}{\beta\,COS\,\theta} \text{ ….. (4)}$$

Where λ is the wavelength of XRD patterns which equal to 0.154 Å ,(β) is the full width at half maximum (FWHM) and (θ) is the Brage diffraction angle in degrees.Eq. (4), where the relation between the crystallite size and (FWHM) is reverse. Decreasing in the crystallite size after doping is evidence on the improvement of the nanocrystal, which indicates that the deposited atoms of these films going towards nanostructure.There was a decrease in the (D) value when WO_3 films doped with Au dopant which indicate to nanoparticales formed which it was resulting from the doping process. To clculated the distance (d) according to Braggs law following eqution (5) **:**

$$\mathbf{n\,\lambda = 2\,d\,Sin\theta \text{ …. (5)}}$$

ISSN: 1813 – 1662 (Print)
E-ISSN: 2415 – 1726 (On Line)

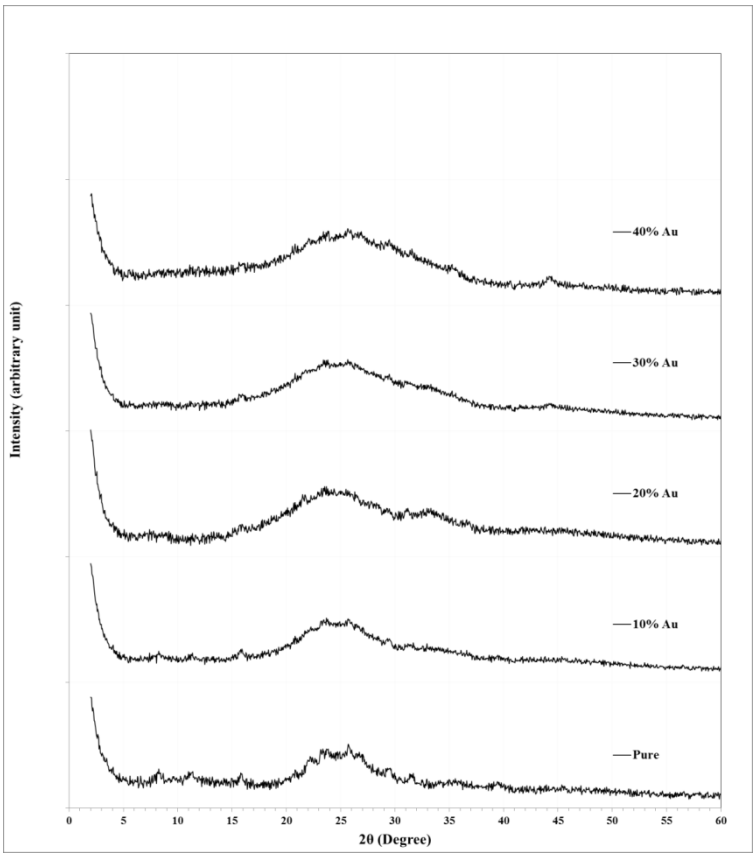

Fig.1 : The XRD pattern of WO_3 doped of Au(0,10,20,30 and 40) wt. % thin films as deposited .

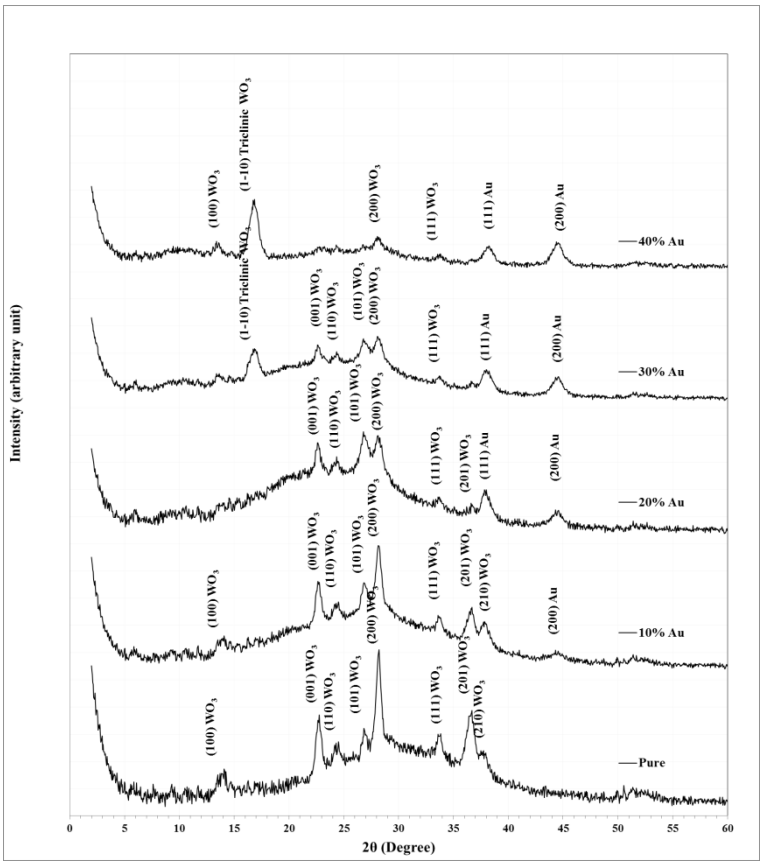

Fig.2: The XRD pattern of WO_3 and doped of Au (0, 10,20,30 and 40) wt. %thin films with annealing temperature at T_a = 400 ˚C.

Table 1: Structural parameters, inter-planar spacing, crystalline size for pure WO_3 and Au thin films at annealing temperature T_a=400˚C.

Au%	2θ (Deg.)	FWHM (Deg.)	d_{hkl} Exp.(Å)	G.S (nm)	d_{hkl} Std.(Å)	hkl
	13.9700	0.6988	6.3342	11.5	6.3203	(100)
	22.7100	0.5430	3.9124	14.9	3.8990	(001)
	24.3300	0.7431	3.6554	10.9	3.6490	(110)
Pure	26.8800	0.4350	3.3142	18.8	3.3184	(101)
	28.1900	0.5320	3.1631	15.4	3.1601	(200)
	33.7400	0.6200	2.6544	13.4	2.6642	(111)
	36.5500	0.8325	2.4565	10.0	2.4550	(201)
	37.8000	0.7658	2.3781	11.0	2.3888	(210)
	13.7500	0.9559	6.4351	8.4	6.3203	(100)
	22.6471	0.6618	3.9231	12.2	3.8990	(001)
	24.3382	0.6618	3.6542	12.3	3.6490	(110)
10%	26.8382	0.8088	3.3192	10.1	3.3184	(101)
	28.1618	0.7353	3.1662	11.1	3.1601	(200)
	33.6029	0.5882	2.6649	14.1	2.6642	(111)
	36.6912	0.8089	2.4474	10.3	2.4550	(201)
	37.7941	0.8089	2.3784	10.4	2.3888	(210)
	44.4118	1.1120	2.0382	7.7	2.0352	(200)
	22.6420	0.5220	3.9240	15.5	3.8990	(001)
	24.3210	0.7220	3.6568	11.3	3.6490	(110)
20%	26.8754	0.9150	3.3147	8.9	3.3184	(101)
	28.1865	0.9700	3.1634	8.4	3.1601	(200)
	33.7344	0.6210	2.6548	13.4	2.6642	(111)
	36.5521	0.8140	2.4563	10.3	2.4550	(201)
	37.8210	0.7540	2.3768	11.1	2.3500	(111)
	44.5300	1.1700	2.0330	7.3	2.0352	(200)
	16.8382	1.1029	5.2612	7.3	5.2170	(1-10)
	22.6471	0.5883	3.9231	13.8	3.8990	(001)
	24.3382	0.6618	3.6542	12.3	3.6490	(110)
30%	26.7647	0.8823	3.3282	9.3	3.3184	(101)
	28.0882	0.8088	3.1743	10.1	3.1601	(200)
	33.6765	0.8088	2.6592	10.3	2.6642	(111)
	38.0147	1.2500	2.3651	6.7	2.3500	(111)
	44.5588	1.1029	2.0318	7.8	2.0352	(200)
	13.5000	0.6540	6.5537	12.2	6.3203	(100)
	16.8000	0.8650	5.2730	9.3	5.2170	(1-10)
40%	28.1643	0.9700	3.1659	8.4	3.1601	(200)
	33.7344	0.6210	2.6548	13.4	2.6642	(111)
	38.3534	0.9150	2.3450	9.2	2.3500	(111)
	44.5213	1.0600	2.0334	8.1	2.0352	(200)

3-2 Electrical properties

Films were tested to confirm their semiconducting behavior .The film is placed on heater and their resistances are measured in the range from 30C˚ up to 200˚C, with step of 10˚C, in the dry air atmosphere. The electrical resistivity of pure WO_3 and doped Au at different concentration films was measured using D.C . Two point probe method . The conductivity follows the relation [15].

$$\sigma = \sigma_{\circ} \exp(-Ea / K_B T) \quad \ldots(6)$$

Where σ is resistivity at temperature T, $\sigma_{\circ}$ is a constant, K_B is Boltzmann constant ($1.38*10^{-23}$ j.sec) , E_a is activation energy for conduction . By taking (Ln) of the two sides of equation (7) we can get :

$$Ln\ \sigma = Ln\ \sigma_{\circ} (-Ea / K_B T) \quad \ldots(7)$$

From determination of the slope we can find the activation energy**:**

$$Ea = K_B \cdot slop \ldots \quad (8)$$

ISSN: 1813 – 1662 (Print)
E-ISSN: 2415 – 1726 (On Line)

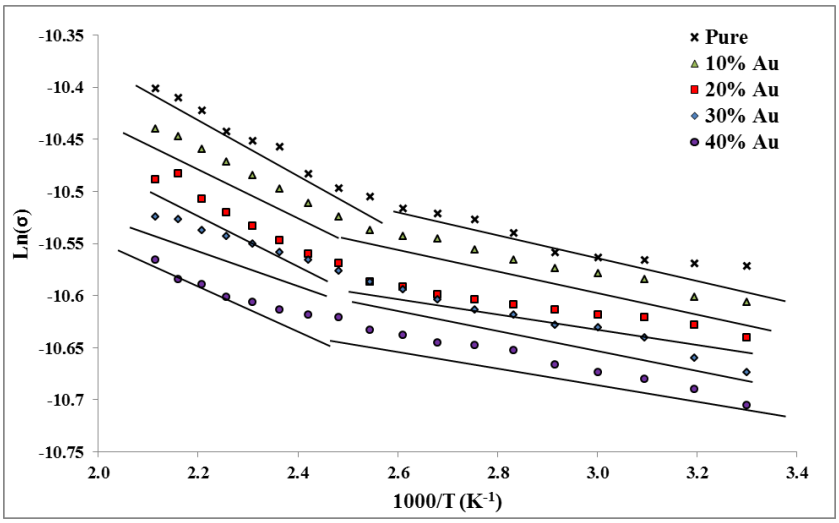

Fig.3:The graph shows the variation of (Lnσ) with (1000/T) for pureWO_3 and doped Au at different concentration on glass substrate as deposited

Fig. 3 shows the variation of (Ln) of conductivity (Ln σ) with 1000/ T $(K)^{-1}$ .For pure and doped Au at different concentration films. Two stages of conductivity throughout the heating temperatures range are noted , first activation energy (E_{a1}) occurs at low temperature , near Fermi level within the range (303-403)K [16-17], while the second activation energy (E_{a2}) K occurs at high temperatures within localized states at the range (403-473)K [16] (see Table 2).The fig.3 shows that there is a decrease in conductivity with the increase in the doping, this is because that the increase of energy gap with increase in the doping, as well as, it can be observed two separated regions throughout the heating temperature range, the first region is at low temperature and the second region is at higher temperature, indicating different conduction mechanisms dominating at specific temperature intervals[18].

Table 2: Values of E_{a1} , E_{a2} and σ_{RT} for pure WO_3 and doped Au thin films at different concentration as deposited.

Au %	E_{a1} (eV)	Range (K)	E_{a2} (eV)	σ_{RT} (Ω^{-1}.cm^{-1})
0	0.008	303-403	0.022	2.33E-05
10	0.008	303-403	0.020	2.30E-05
20	0.006	303-403	0.021	2.18E-05
30	0.009	303-403	0.031	2.10E-05
40	0.008	303-403	0.021	2.26E-05

Fig. 4 shows the variation of (Ln) of conductivity (Ln σ) with 1000/ T $(K)^{-1}$ .For pure and doped Au at different concentration films. Two stages of conductivity throughout the heating temperatures range are noted , first activation energy (E_{a1}) occurs at low temperature , near Fermi level within the range (303-393)K [16-17], while the second activation energy (E_{a2}) K occurs at high temperatures within localized states at the range (393-473)K [16] (see Table 3). The variation of activation energies for annealing temperature at 400C˚ on a glass substrate is shown in fig.4. The figure shows that conductivity of the annealed films is larger. This is because with the increase in annealing temperature, grain size increases resulting in a decrease in grain boundaries and associated impedance to the flow of charge carriers [19]. Such a behavior is favorable for gas sensor applications of these films [20].

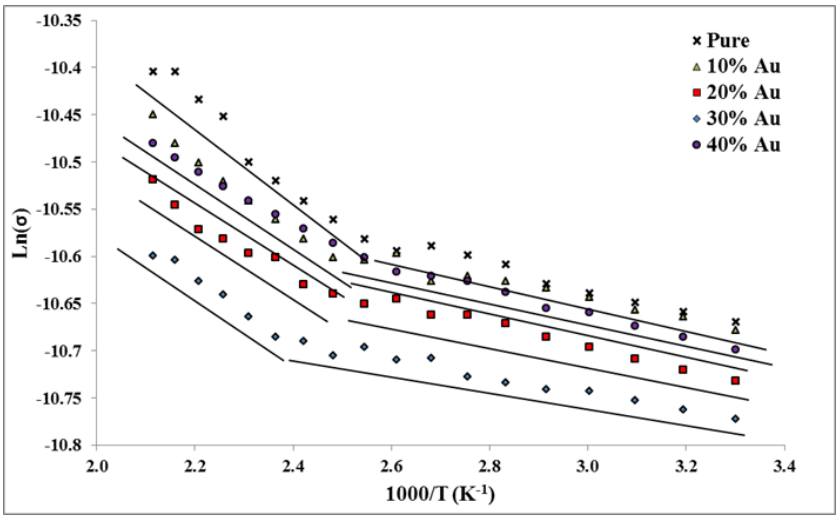

Fig.4: The graph shows the variation of (Lnσ) with (1000/T) for pureWO_3 and doped Au thin films at different concentration on glass substrate at temperature 400˚C.

Table 3: Values of E_{a1} and E_{a2} σ_{RT} for pure and doped Au thin films at different concentration with annealing temperature 400˚C.

Au %	E_{a1} (eV)	Range (K)	E_{a2} (eV)	σ_{RT} ($\Omega^{-1}.cm^{-1}$)
0	0.011	303-393	0.039	2.56E-05
10	0.009	303-393	0.036	2.48E-05
20	0.010	303-393	0.027	2.39E-05
30	0.008	303-393	0.023	2.31E-05
40	0.011	303-393	0.024	2.24E-05

The variation of carriers concentration (n_H) and Hall mobility (μ_H) of un-doped WO3 and doped with different concentration thin films of Au before and after annealing at 400˚C are shown Fig. (5-8). Hall measurements show that all these films have a negative Hall coefficient (n-type charge carriers) this results was agreement with [21]. This is attributed to following two reasons [22].

i. The number of electrons excited above the conduction bands is larger than the number of holes excited below the valance band.

ii. The life time of free electrons excited from negative defect state is higher than the life time of free holes excited from positive defect state.

It's clear from (see Tables 3 and 4) that the carrier concentration increases with dopant ratio while there was decreasing in carrier mobility (μ_H) with dopant concentration and the doping process did not affect on the type of the charge carriers. It is due to decrease the disorder of the crystal lattice, which causes decreases in phonon scattering and ionized impurity scattering and results in a decrease in mobility [23].

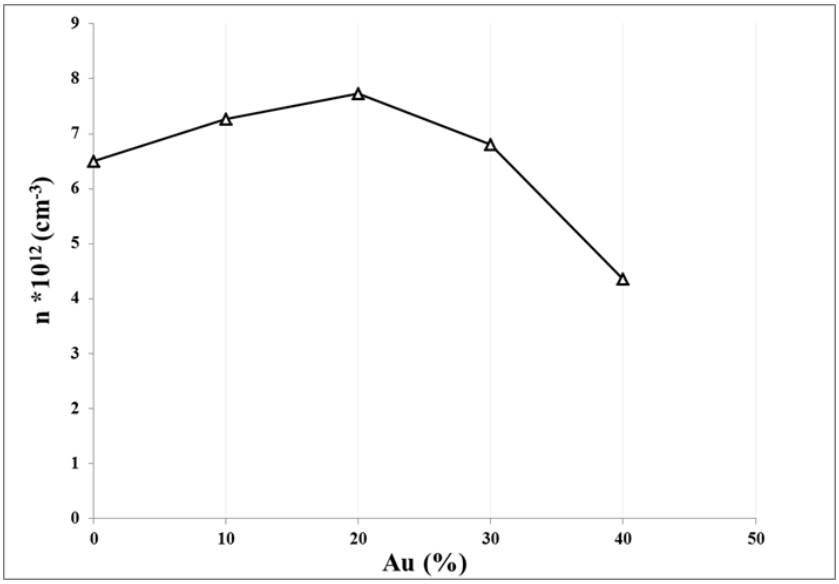

Fig.5: Variation of carrier concentration (n) with dopant ratio of Au (0, 10, 20, 30 and 40) wt. % thin films as deposited

ISSN: 1813 – 1662 (Print)
E-ISSN: 2415 – 1726 (On Line)

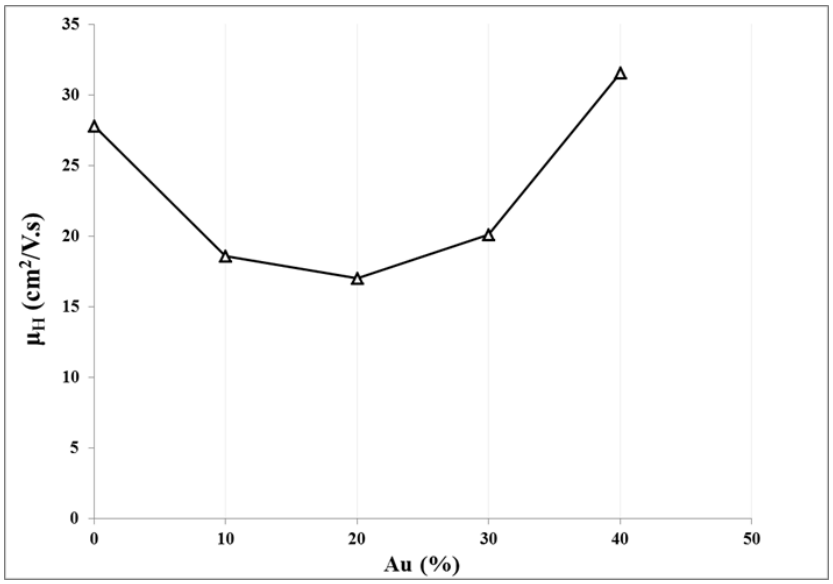

Fig.6: Variation of Mobility (μ_H) with dopant ratio of Au (0,10, 20, 30 and 40) % wt. thin films as deposited

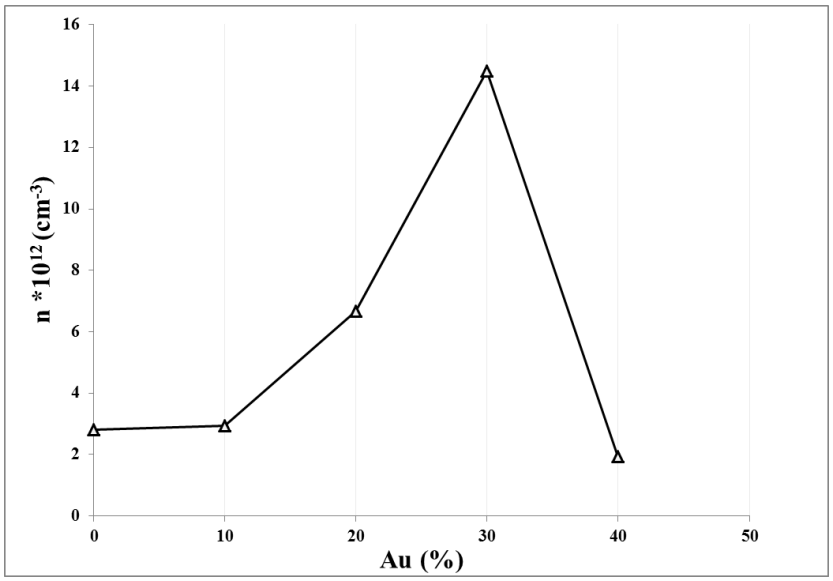

Fig.7: Variation of carrier concentration (n) with dopant ratio of Au (0, 10, 20, 30 and 40) %wt. thin films at annealing temperature = 400 C°

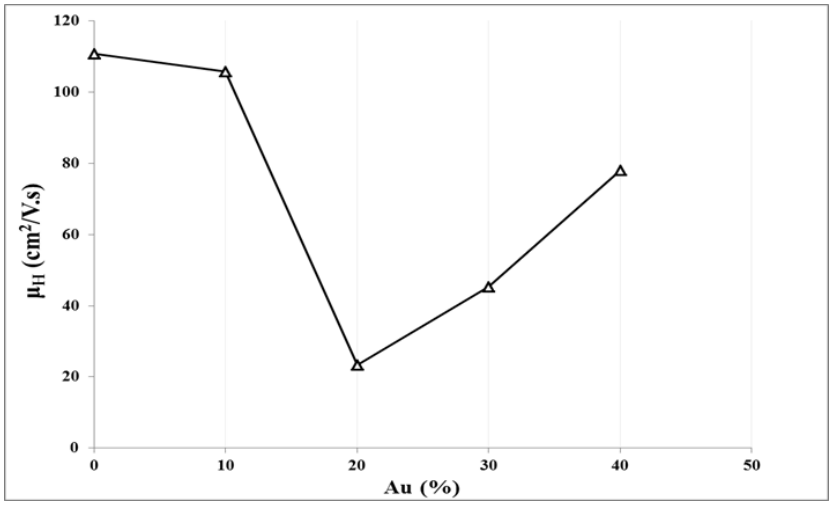

Fig.8: Variation of Mobility (μ_H) with dopant ratio of Au (0,10, 20, 30 and 40) % wt. thin films at annealing temperature = 400 C°

Table 4: Hall measurements results of WO_3 thin films at different Au dopant ratio (0, 10, 20, 30 and 40) %wt. as deposited

Au %	σ_{RT} ($\Omega^{-1}.cm^{-1}$)	R_H	n (cm^{-3})*10^{13}	μ_H (cm^2/v.sec)
0	2.90E-05	960500	6.507	27.85
10	2.16E-05	860500	7.263	18.59
20	2.11E-05	809000	7.726	17.06
30	2.19E-05	919200	6.799	20.13
40	2.20E-05	1436000	4.352	31.59

Table 5: Hall measurements results of WO_3 thin films at different Au dopant ratio (0, 10, 20, 30 and 40) % wt.at annealing temperature = 400C°

Au %	σ_{RT} ($\Omega^{-1}.cm^{-1}$)	R_H	n (cm^{-3})*10^{13}	μ_H (cm^2/v.sec)
0	4.99E-05	2220000	2.815	110.78
10	4.99E-05	2120000	2.948	105.79
20	2.49E-05	936000	6.677	23.31
30	1.05E-04	431000	14.501	45.26
40	2.40E-05	3250000	1.923	78.00

4- Conclusion

The WO_3 thin film with different doping concentration of Au nanoparticles (0,10,20,30 and 40) wt.% based on chemical spray pyrolysis deposition have been prepared on glass substrate at T_s =250˚C successfully. The X-ray diffraction pattern of WO_3 :Au at substrate temperature 250˚C show amorphous, but with annealing temperature the structure will became a polycrystalline for different doping concentration of gold nanoparticles all prepared films have two activation energies Ea_1 and Ea_2 at range (303-473)K these activation energies decrease with the increasing of Au concentration. And the D.C conductivity for all films at 250C˚ and 400C˚ decreases with increase doped by Au for all concentration

Reference

[1] Dugleux, P. and de alameda marques, S., " **preparation of metal powders of groups VI and VIII (Fe, Co, Ni) by the vapor phase reduction of their chlorides pure or in binary mixtures**", Powder Technology,.27 (1), 45–52,(1980) .

[2] J. Jakobi, A. Menéndez-Manjón, V.S.K. chakravadhanula, L**.** Kienle, P. Wagener, S. Barcikowski, Nanotech **"stoichiometry of alloy nanoparticles from laser ablation of Pt Ir in acetone and their electrophoretic deposition on Pt Ir electrodes**" 22, 145601-145607, (2011).

[3] J. Jakobi,S. Petersen, A. Menéndez-Manjón, P. Wagener, S. Barcikowski, "**magnetic alloy nanoparticles from laser ablation cyclopentanone and their embedding in to aphotoresist**", langmuir ,26(10), 6892–6897,(2010).

[4] W.G. Zhang, Z.G. Jin, "**research on successive preparation of nano-FeNi alloy and its ethanol sol by pulsed laser ablation**"Sci. China Ser. B,(47), 159-165,(2004)

[5] D. Poondi, T. Dobbins, J. Singh," **anovel laser liquid soild interaction**
technique for synthesis of silver, nickel and immiscible silver nickel alloy from liquid processors", J. Mater. Sci., 35(24), 6237-6243, (2000).

[6] Lai, Wei Hao, "**Synthesis of tungsten oxide particles by chemical deposition method.** " Materials transactions 48 (6) , 1575-1577, (2007).

[7] Dong-myong,"**Full Open Access Journals Have Increased Impact Factors Molecular** "Diversity Preservation International, 12 (5), 519-528,(2005).

[8] Akl et al., "**microstructural and electrical properties of (WO3) 1-x (MoO3) x thin films synthesized by spray pyrolysis technique** " Journal of Material Sciences (2321 – 6212), (2016) .

[9] Ganbavle, "**structural, optical, electrical and dielectric properties of the spray deposited WO_3 thin films**" journal of materials engineering and performance, 23 ,1204-1213, (2014).

[10] H .Rezvani, "**the effect of deposition parameters on the sensing behaviors of the Sno2:Cu nanostructure thin films including Co_2 gas sensor**" Indian journal of science, 3(6), 0974-6846, (2010).

[11] Lijun Li, Kera, a- Zheng Tang, Ziqiang Zhu, and Qing Wan,"**room temperature ferromagnetism properties of Cu doped nanowires**" Journal of Applied physics, 107, 014303, (2010) .

[12] Jae Cheon Sohn, Sung Eun Kim, Zee Won Kim, and Yu "**transactions on electrical and electronic materials**, 10, 4, (2009).

[13] Joseph, V.Mathew, and K.E Ibrahim, Chinese Journal of physics, 45(1),(84-97) (2007).

[14] Sitrotin, Y. and M. Shaskolskaya, "**Fundamental of crystal physics**", Mir publishers, Moscow, (1982) .

[15] P.S. Kireev, "**Semiconductor Physics**", Translated from Russian by M. Samokhvalov, MIR publishers, Moscow (1978).

[16] Yadav, A. A. and E.U. Masumdar, "**Optical and electrical transport properties of spray deposited $CdS_{1-x}Se_x$ thin films**", Journal of Alloys and Compounds, 505, (787–792), (2010).

[17] Prabahar, S., N. Suryanarayanan and D. Kathirvel," **electrical and photoconduction studies on chemical bath deposited cadmium sulphide thin films**", Chalcogenide Letters, 6 (11), (577-581), (2009).
[18] A. Salah Hamead, "**electronic properties of the A-Ge/C-Si Heterojunction**", M.SC., Thesis, Baghdad University, (2009).
[19] R.S. Vemuri, K. Kamala Bharathi, S.K. Gullapalli, C.V. Ramana, Appl. Mater.
Interfaces 9, 2623 (2010).
[20] M.G. Hutchins, O. Abu-Alkhair, M.M. El-Nahass, K. Abdel-Hady," **electrical conduction mechanisms in thermally evaporated tungsten trioxide WO_3 thin films**" J. Phys. Condens. Matter 18, 9987 (2006).
[21] Ganbavle et al., "**Structural, Optical, Electrical, and Dielectric Properties of the Spray-Deposited WO3 Thin Films**", Springer, Journal of materials engineering and performance, 23, 1204-1213, (2014).
[22] S. K. and S. G. Vijaykumar.B.Chanshetty1, "**Surface Morphology Studies and Thermal analysis of V2O5 doped polyaniline composites**," Int. J. Eng. Res. Appl., 2(5), 611–616, (2012).
[23] H. Kim, C. M. Gilmore, "**electrical , optical and structural properties of indium tin oxide thin films for organic light emitting devices**" J. Appl. Phys., 86 (11) 6451– 6461, (1999).

تاثير الجزيئات النانوية للذهب على الخواص التركيبية والكهربائية لاغشية اوكسيد التنكستن الرقيقة

نيران فاضل عبد الجبار[1] ، عصام محمد ابرهيم[2] ، عبير حاتم فزع[1]

[1]قسم الفيزياء ، كلية التربية للعلوم الصرفة ، جامعة تكريت ، تكريت ، العراق

[2]قسم الفيزياء ، كلية العلوم ، جامعة بغداد ، بغداد ، العراق

الملخص

أُستخدمت طريقة التحليل الكيميائي الحراري عند حرارة القواعد250°Cولدنت هذه الاغشية لمدة ساعة بحرارة400°C, لترسيب اغشية رقيقة من اوكسيد التنكستن بتراكيز تطعيم مختلفة من جزيئات الذهب النانوية (0,10,20,30 and 40) wt.% ,على قواعد زجاجية وبسمك 100 nm , أُجريت الفحوصات التركيبية والكهربائية وتبين من الخصائص التركيبية للاغشية المحضرة على الارضيات الزجاجية باستخدام حيود الاشعة السينية XRD انها تمتلك تركيب غير متبلور عند حرارة250°C,وتمتلك تركيب متعدد التبلور وبالتركيب السداسي لاوكسيد التنكستن وبالاتجاه السائد (200)وان اغشية WO_3 المشوبة بالذهب لها تركيب مكعبي الطور عند حرارة تلدين 400C° , كما نوقشت ميكانيكية التوصيلية المباشرة لغشاء التنكستن النقي والمشوب بالذهب بتراكيز مختلفة (0,10,20,30 and 40) wt.% ولمدى (303-473) K,هناك نقصان في التوصيلية مع زيادة تركيز التطعيم , وبينت قياسات هول ان كل الاغشية تمتلك معامل هول سالب و(n_H) تزداد مع زيادة نسبة التشويب (Au) ونقصان في تحركية الحاملات (μ_H) مع زيادة نسبة التطعيم (Au).